

# The warm absorber of the Seyfert 1 galaxy H1419+480

X. Barcons<sup>\*</sup>, F.J. Carrera, M.T. Ceballos

*Instituto de Física de Cantabria (CSIC-UC), 39005 Santander, Spain*

March 2003

## ABSTRACT

The bright Seyfert 1 galaxy H1419+480 ( $z \sim 0.072$ ), whose X-ray colours from earlier HEAO-1 and *ROSAT* missions suggested a complex X-ray spectrum, has been observed with *XMM-Newton*. The EPIC spectrum is well fit by a power-law with photon index  $\Gamma = 1.84 \pm 0.01$  and an Fe K $\alpha$  line of equivalent width  $\sim 250$  eV. At low energies, an intrinsic OVII K-edge is unambiguously detected with a  $\tau_{OVII} \sim 0.45$ , but no OVIII absorption edge is detected to within sensitive limits. The absorption features are equally well fit by an ionised absorber ( $\xi \sim$  a few) with column density  $N_H \sim 2.5 \times 10^{21} \text{ cm}^{-2}$  for solar abundances. We find that the flux of this source has varied with respect to earlier *ROSAT* observations, and there are hints that the warm absorber was weaker or absent in that previous observation. An IUE spectrum of this source shows an associated and variable (within a year) CIV absorber outflowing with a velocity  $\sim 1800 \text{ km s}^{-1}$ . We argue that both the UV and X-ray absorption can be consistently modelled in terms of photoionised pc-scale gas blobs at  $\sim 100$  pc distance from the nucleus.

**Key words:** X-rays: galaxies, galaxies: active

## 1 INTRODUCTION

X-ray spectral studies of radio-quiet Active Galactic Nuclei (AGNs), reveal very often the presence of ionised material. This was first noted by Halpern (1984), based on *Einstein* IPC data, where it was also noted that these absorbers vary. Evidence for ionized absorption along the line of sight was provided by Nandra & Pounds (1992), based on the detection of an absorption edge in *ROSAT* observations of the Seyfert 1 galaxy MCG-6-30-15. Fabian et al (1994) were able to disentangle the OVII and OVIII K-edges of this warm absorber using the much better spectral resolution of *ASCA*.

In the years that followed, it became evident that warm absorbers are ubiquitous among Seyfert 1 galaxies. Reynolds (1997) and George et al (1998) showed that more than 50% of Seyfert 1s contain a warm absorber. These are produced by partially ionized gas with total column density in the range  $N_H \sim 10^{21} - 10^{23} \text{ cm}^{-2}$ , probably located at or outside the Broad Line Region (Reynolds & Fabian 1995).

Detailed studies of particular AGN which exhibited X-ray ionized absorption features also demonstrated that there is often an associated (ie, related to the AGN) absorber in the ultraviolet band, often showing up as a CIV  $\lambda\lambda 1548, 1550$  absorption line (Mathur 1994, Mathur et al 1994, Mathur, Elvis & Wilkes 1995). The same photoionized outflowing gas can provide the UV absorption lines and the ionized absorption features seen in X-ray spectra. In

a more recent compilation Crenshaw et al (1999) found in a systematic study of UV absorption lines towards nearby radio-quiet AGN, that *all* objects showing UV associated absorption systems have a corresponding warm absorber in the X-rays.

Variability has also been often found in these warm absorbers. Fabian et al (1994) reported different absorption optical depths in the best-studied warm absorber towards MCG-6-30-15. Later, Otani et al (1996) showed, using a 4-day long ASCA observation of this particular Seyfert 1, that the OVIII K edge (at a rest frame energy of 0.871 keV) varied on scales of  $\sim 10$  ks, while the OVII K-edge (at a rest frame energy of 0.739 keV) remained constant. Otani et al (1996) interpreted this in terms of two different ionized absorbers, a high ionisation (OVIII) absorber located within the BLR and a lower ionisation absorber (OVII) probably associated to the Narrow Line Region (NLR).

H1419+480 was discovered in the Modulation Collimator - Large Area Sky Survey (MC-LASS) conducted with the HEAO-1 observatory (Wood et al 1984). The inferred 2-10 keV flux was  $\sim 2 \times 10^{-11} \text{ erg cm}^{-2} \text{ s}^{-1}$ , assuming a power law spectrum with a canonical  $\Gamma = 1.7$  (Ceballos & Barcons 1996). Although the modulation collimator helped to pin down the position of the X-ray source, the flux could be severely affected by the contribution of unresolved sources within the collimator field of view. A similar example has been recently reported by Barcons, Carrera & Ceballos (2003). The *ROSAT* All-Sky Survey (RASS) also detected this source (see Schwope et al 2000), with

<sup>\*</sup> E-mail: barcons@ifca.unican.es

a 0.5-2 keV flux (corrected for Galactic absorption) of  $\sim 7 \times 10^{-12}$  erg cm $^{-2}$  s $^{-1}$  and an additional *PSPC* observation conducted in 1992 found a flux of  $\sim 3 \times 10^{-12}$  erg cm $^{-2}$  s $^{-1}$ . In both cases the *PSPC* hardness ratio was  $\sim 0$  which excluded a significant photoelectric absorption by cold gas.

Remillard et al (1993) identified H1419+480 with a broad-line type 1 AGN at  $z = 0.072$  ( $RA = 14^h 21^m 29.60^s$ ,  $DEC = +47^\circ 47' 27''$ ). Appendix A presents our own optical spectroscopic observations of H1419+480, which confirm that this source is a broad-line AGN with  $z = 0.07229$ , as derived from the [OIII] emission doublet.

Ceballos & Barcons (1996) analyzed a sample of sources detected both in the MC-LASS sample and by *ROSAT* (which included H1419+480). The large decrement of the flux from hard to soft X-rays is suggestive of heavy photoelectric absorption, which is at odds with the value reported for the *PSPC* hardness ratio. This was interpreted by Ceballos & Barcons (1996) as evidence for complex absorption, that could be modelled either in terms of an ionized absorber or in terms of a partial covering cold absorber.

In this paper we present *XMM-Newton* EPIC observations of H1419+480. We find that the source has changed the soft X-ray flux again and that its 2-10 keV flux is almost a factor 3 lower than the HEAO-1 one. A warm absorber is unambiguously seen in the *XMM-Newton* data through the OVII absorption edge, but we argue that this warm absorber was weaker or absent in the previous pointed *ROSAT* observation. An associated CIV absorption line is seen in an *International Ultraviolet Explorer* (*IUE*) spectrum of this source taken more than 20 years ago, but it is not seen in a similar observation taken one year later. We find that the gas that causes X-ray and associated UV absorption can be consistently modelled in terms of photoionised pc-scale clouds, 100 pc away from the nucleus.

## 2 X-RAY PROPERTIES

### 2.1 *XMM-Newton* observations

H1419+480 was observed by *XMM-Newton* (Jansen et al 2001) for 27 ks on the 27th of May of 2002, during revolution 451 (obsid=0094740201), as part of the Guaranteed Time programme of the Survey Science Centre. In this paper we analyze only the data obtained by the EPIC MOS (Turner et al 2001) and EPIC pn (Strüder et al 2001) cameras. The source is clearly detected by the RGS spectrographs (den Herder et al 2001), but it is far too faint to deliver any scientifically interesting results. The OM (Mason et al 2001) was used to obtain images in the filters U, B and UVW1.

All 3 EPIC cameras had the 'Thin 1' filter on, and they were operated in partial window mode (MOS1 and MOS2) and small window mode (pn). Exposure times (excluding overheads) were 13 ks for the MOS cameras and 20 ks for the pn camera. However, most of the exposure time was lost due to high background flaring. After cleaning out these intervals, good-time intervals of  $\sim 8$  ks were left for the MOS1 and MOS2 detectors, and 3 ks were left for the pn detector. Fortunately H1419+480 is bright enough (5 cts/s in the EPIC pn camera) to provide a large enough number of counts for spectral analysis.

Event files for the 3 EPIC detectors were taken from

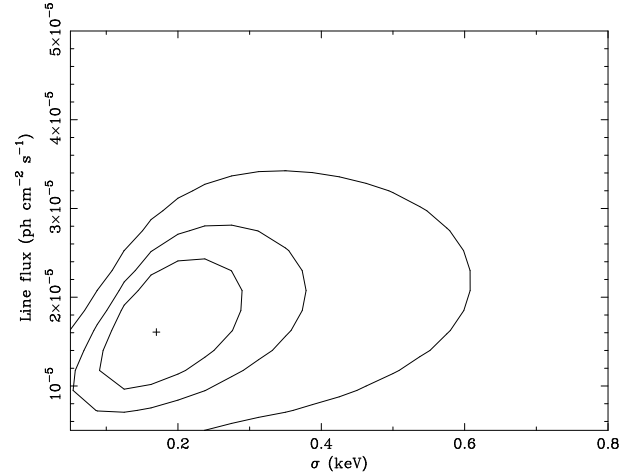


**Figure 1.** Confidence contours (1,2 and 3 sigma) for the flux versus dispersion of the Fe line

the distributed pipeline products, which were obtained by processing the observation data file with SAS v5.3.3. We filtered out high-background intervals, keeping only the most reliable single and double events and, in the case of EPIC pn, those with FLAG=0. Calibration matrices were generated by using SAS v5.4.1, which we found to solve some problems at energies 0.5-1 keV with respect to the SAS v5.3.3 calibration.

X-ray spectra for H1419+480 and background, were extracted from the 3 EPIC cameras. The background spectrum was extracted from regions in the same chip as the source one but not illuminated by H1419+480. This was also done in the MOS data, as opposed to source-free regions in the outer chips, to prevent vignetting affecting the background subtraction. The source plus background pn, MOS1 and MOS2 spectra were binned individually into bins containing at least 20 counts each. To fit spectra models to these data, **xspec** version 11.2.0 was used (Arnaud 1996). Bins outside the 0.2-12 keV bandpass were ignored. At the time of performing this analysis, a calibration problem of the MOS detectors below 0.5 has been reported, being probably related to the redistribution matrix at very low energies. We have exercised a few fits ignoring all MOS1 and MOS2 data below 0.5 keV, but the results remained mostly unchanged, with best-fit parameters to spectral models falling between the 90% error bars of the fitted ones including these low-energy datapoints. The values presented in this paper are those obtained by fitting the data down to 0.2 keV for all 3 detectors.

### 2.2 The Fe line

We first fit the 2-12 keV spectrum to determine the underlying continuum. A single power law fit gave  $\chi^2 = 305.96$  for 311 degrees of freedom (two parameters fitted), but with obvious residuals around 6 keV. Adding a redshifted gaussian emission line improved the fit substantially to  $\chi^2 = 290.17$  for 308 degrees of freedom. The F-test assigned a significance to the detection of this line of 99.90%. Parameters resulting from the fit are listed in table 1, while fig. 1 shows the confidence contours in the line flux versus line dispersion parameter space. The line equivalent width derived from these parameters is  $240^{+125}_{-110}$  eV. All parameters are entirely con-

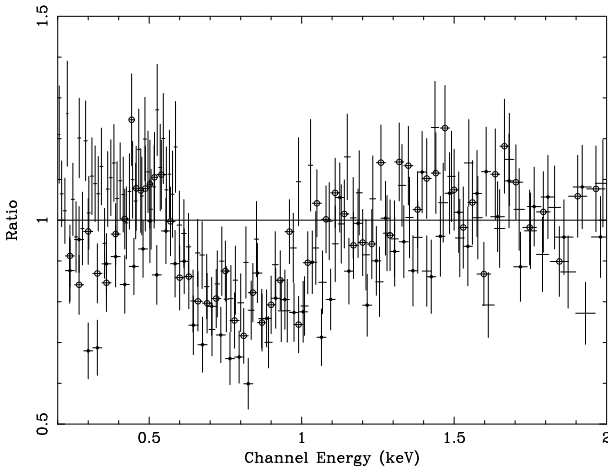


**Figure 2.** *XMM-Newton* EPIC spectral ratio of data to a model without absorber (see text for details). Crosses are from EPIC pn, filled circles from EPIC MOS1 and hollow circles from EPIC MOS2. The data points have been binned into 100 count bins for illustration purposes only.

sistent with those from other Seyfert 1 galaxies (Nandra & Pounds 1994). The EPIC pn spectrum shows a hint of a residual towards low energies, reminiscent of relativistic effects in a disk line, but since the MOS1 and MOS2 spectra do not show such residuals we do not explore this point any further. This emphasizes again the importance of calibration in the detection of weak features (such as relativistic line profiles) in moderate signal-to-noise data.

### 2.3 The ionised X-ray absorber

We then extend the fit to 0.2 keV, including photoelectric absorption from the Galaxy ( $N_H = 1.65 \times 10^{20} \text{ cm}^{-2}$ ), and freezing the line energy and dispersion to their fitted values. The fit is not good, with  $\chi^2 = 1203.94$  for 835 degrees of freedom. There are obvious residuals that call for an absorption edge, as shown in fig. 2. As suggested in Ceballos & Barcons (1996) we tried a partial covering model with a cold absorber, but the improvement of the fit was not significant ( $\chi^2 = 1196.48$ ).

Instead, adding a redshifted absorption edge, the  $\chi^2$  improves dramatically to  $\chi^2 = 979.85$  for 833 degrees of freedom. The F-test significance of this edge is virtually 100% (within  $\sim 10^{-39}$ ). The edge energy at the redshift of H1419+480 is entirely coincident with that of the OVII K-edge expected at 0.739 keV (see table 1). The relative velocity of the absorbing material with respect to an assumed redshift of  $z = 0.07229$  is  $-4500^{+4500}_{-9000} \text{ km s}^{-1}$ . This is consistent with the absorbing material being associated to the Seyfert 1 galaxy itself. The resulting fitted spectrum is shown in fig. 3

Although there are no obvious residuals, we have also tried to find a second absorption edge, perhaps the OVIII K-edge at 0.871 keV. The  $\chi^2$  only improves modestly to  $\chi^2 = 972.55$  for 831 degrees of freedom, with an F-test significance of the additional edge of only 95%. Further, the edge energies at the rest-frame of H1419+480 are now  $0.70^{+0.02}_{-0.02} \text{ keV}$  and  $0.81^{+0.05}_{-0.04} \text{ keV}$ , both significantly redshifted with respect to the OVII and OVIII K absorption edges at velocities

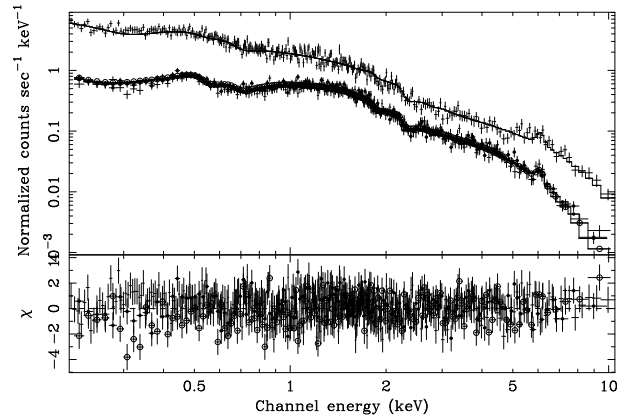


**Figure 3.** *XMM-Newton* EPIC spectrum and residuals with respect to the fit reported in table 1. Crosses are from EPIC pn, filled circles from EPIC MOS1 and hollow circles from EPIC MOS2.

**Table 1.** X-ray spectral parameters of H1419+480. All errors are 90% confidence for 1 interesting parameter.

Parameter	Value	Units
<b>zgauss</b>		
$E_{line}^*$	$6.52^{+0.12}_{-0.11}$	keV
$\sigma_{line}^*$	$0.17^{+0.14}_{-0.06}$	keV
$F_{line}$	$(1.7^{+0.8}_{-0.8}) \times 10^{-5}$	$\text{ph cm}^{-2} \text{ s}^{-1}$
<b>zpowerlaw</b>		
$\Gamma$	$1.84^{+0.02}_{-0.01}$	
$A_\Gamma$	$(2.53 \pm 0.03) \times 10^{-3}$	$\text{ph cm}^{-2} \text{ s}^{-1} \text{ keV}^{-1}$
<b>zedge</b>		
$E_{edge}$	$0.727^{+0.012}_{-0.023}$	keV
$\tau$	$0.46^{+0.06}_{-0.06}$	

\* The parameter has been obtained in a fit to the 2-12 keV band, and then frozen at this value.

$\sim -15000^{+8000}_{-11000} \text{ km s}^{-1}$  and  $-20000^{+17000}_{-12000} \text{ km s}^{-1}$ . Similar apparently redshifted absorption edges have been already seen in higher resolution RGS spectra of MCG-6-30-15 and Mkn 766 (Branduardi-Raymont et al 2001), and attributed either to broad emission lines (Branduardi-Raymont et al 2001, Mason et al 2003) or to a dusty warm absorber (Lee et al 2001). However, given the low level of significance of the second edge, together with the discovery of an associated CIV absorption system outflowing from H1419+480 at a much more modest velocity (see later) we do not pursue this two edge solution any further. Instead, a  $3\sigma$  upper limit to the depth of the OVIII edge of around  $\tau_{OVIII} \sim 0.20$  can be derived by freezing its edge energy 0.871 keV.

The dominance of the OVII edge over the OVIII edge probably places the absorber outside the BLR and suggests a moderate ionisation parameter. To further test this point, we modeled the absorption using the `absori` routine under `xspec`, assuming solar abundances. We assume that the absorber is at the H1419+480 redshift ( $z = 0.07229$ ) and we further assume a power law continuum ionising spectrum with  $\Gamma = 1.84$ . Table 2 shows the parameters of the fit for a range of *assumed* absorber temperatures. Indeed the fit marginally improves when the absorber temperature

**Table 2.**  $\chi^2$  for 832 degrees of freedom and parameters fitted to an ionized absorber as a function of its temperature. All errors are 90% confidence for 1 interesting parameter. The last two columns indicate the expected CIV and HI column densities respectively (see sect 4 for details).

$T_{abs}$ (K)	$\chi^2$	$\xi$ (erg cm s $^{-1}$ )	$N_H$ (cm $^{-2}$ )	$N_{\text{CIV}}$ (cm $^{-2}$ )	$N_{\text{HI}}$ (cm $^{-2}$ )
$1 \times 10^4$	1003.11	$6.7^{+3.5}_{-2.0}$	$(2.4 \pm 0.3) \times 10^{21}$	$3.6 \times 10^{17}$	$1.6 \times 10^{18}$
$3 \times 10^4$	1005.97	$3.8^{+1.8}_{-0.9}$	$(2.3 \pm 0.3) \times 10^{21}$	$1.6 \times 10^{17}$	$5.0 \times 10^{17}$
$1 \times 10^5$	998.36	$3.7^{+1.2}_{-0.8}$	$(2.4 \pm 0.3) \times 10^{21}$	$3.5 \times 10^{16}$	$2.6 \times 10^{16}$
$3 \times 10^5$	991.83	$2.0^{+0.5}_{-0.3}$	$(2.5 \pm 0.3) \times 10^{21}$	$1.8 \times 10^{15}$	$3.0 \times 10^{15}$
$1 \times 10^6$	990.65	$1.0^{+0.2}_{-0.2}$	$(2.6 \pm 0.3) \times 10^{21}$	$1.9 \times 10^{14}$	$5.3 \times 10^{14}$
$3 \times 10^6$	982.52	$1.3^{+0.4}_{-0.3}$	$(2.7 \pm 0.3) \times 10^{21}$	$5.7 \times 10^{11}$	$1.3 \times 10^{14}$

grows, reaching similar values as the fit with one single OVII edge. Formally, the best fit is around  $T_{abs} \sim 7 \times 10^5$  K but with very large errors. The temperature is very poorly determined as shown by the slow variation of the  $\chi^2$ . In any case, the total absorbing column is fairly stable at around  $N_H \sim 2.5 \times 10^{21}$  cm $^{-2}$  and the ionisation parameter  $\xi$  is moderate ( $\sim$  a few) in all cases.

#### 2.4 Comparison to previous X-ray observations

Using the best-fit model with a single absorption edge, we compute the flux of H1419+480, corrected for Galactic absorption, to be  $4.5 \times 10^{-12}$  erg cm $^{-2}$  s $^{-1}$  in the 0.5-2 keV band and  $7.4 \times 10^{-12}$  erg cm $^{-2}$  s $^{-1}$  in the 2-10 keV band. Adopting currently fashionable cosmological parameters ( $H_0 = 70$  km s $^{-1}$  Mpc $^{-1}$ ,  $\Omega_m = 0.3$  and  $\Omega_\Lambda = 0.7$ ), the luminosity of H1419+480 is  $5.7 \times 10^{43}$  erg s $^{-1}$  in the 0.5-2 keV band and  $9.3 \times 10^{43}$  erg s $^{-1}$  in the 2-10 keV band.

The *XMM-Newton* 2-10 keV flux is almost a factor of 3 smaller than the HEAO-1 flux, a fact that can be at least in part explained by source confusion in the HEAO-1 collimators (see Barcons et al 2003 for a discussion on a similar situation for another source).

There are two *ROSAT* observations of H1419+480 recorded from this source: one from the *RASS* (reported in Schwope et al 2000) and a second one performed on January 1992 (observation sequence ROR700038), used in Barcons & Ceballos (1996). Table 3 lists some data of these observations, along with expectations from the *XMM-Newton* observation. We have folded our best-fit model to the *XMM-Newton* data through the *ROSAT* PSPC-B response to compute the expected spectral shape in the *ROSAT* observations and to convert count rates to fluxes.

The first obvious conclusion is that the 0.5-2 keV flux has changed significantly between the 3 different observations. The expected spectral shape in the *ROSAT* observations appears similar (but not identical) to the measured one. The PSPC Hardness and Softness Ratios (see caption of table 3 for definitions) expected in the *ROSAT* data from our best-fit model to the *XMM-Newton* spectrum have been computed with and without the OVII absorption edge. If anything,  $SR_1$  and  $SR_2$  in the 1992 observation appear to be more consistent with the absence (or weakening) of the optical depth of the OVII edge. Indeed, a steepening of the underlying spectral index to  $\Gamma = 2$  while preserving the absorber's parameters would rise  $SR_2$  to 0.66, but then

$SR_1 = 2.3$ , i.e., further away from the measured value of 1.6. Cold absorption added into the model could do the job, but then we are invoking a variable absorber too. In summary, comparison of the *XMM-Newton* to earlier *ROSAT* data shows not only variable flux for H1419+480, but also a varying absorber.

### 3 AN ASSOCIATED CIV ABSORBER

The compelling evidence that X-ray warm absorbers share a common origin with associated narrow-line absorbers in the UV (Crenshaw et al 1999) urged us to search in available archives for UV spectroscopic observations of H1419+480. Unfortunately the *Hubble Space Telescope* (*HST*) has not observed this object with any of the UV spectrographs, but the *IUE* did observe it several times. Table 4 lists the observations conducted with the SWP short wavelength camera (operated at low dispersion  $\sim 6$  Å), which encompass both the Ly $\alpha$   $\lambda 1216$  and the CIV  $\lambda 1549$  emission lines. We analyzed the INES (IUE Newly Extracted Spectra) data from both of these observations.

Fig. 4 shows the spectra obtained by *IUE* during both observations, around the CIV emission line. Only channels which have not been flagged for any reason are plotted. The overall flux shift between both spectra could be either true variability or a calibration problem. The most obvious discrepancy between both spectra occurs at around  $\lambda \sim 1651$  Å, where the earlier observation (SWP17265) shows a dip that could be an absorption line.

To further investigate this, and keeping in mind that detecting absorption lines on top of emission lines is a difficult task, we have taken the 8 channels ranging from 1643 to 1656 Å in the SWP17265 spectrum. A linear function was fitted to that range, resulting in a  $\chi^2 = 17.65$  for 6 degrees of freedom. Multiplying by a gaussian absorption line and freezing its width to the resolution of the spectrograph (i.e., searching for an unresolved line) the  $\chi^2$  improved to  $\chi^2 = 0.99$  for 4 degrees of freedom. The F-test significance of that negative feature is 99.7% ( $\sim 3\sigma$ ). The central wavelength is  $\lambda_{abs} = 1651.1 \pm 0.5$  Å, corresponding to an outflowing velocity of  $\sim 1800$  km s $^{-1}$ . The equivalent width is also very uncertain, due to the poor sampling, but formally the best fit is  $3^{+0.7}_{-0.9}$  Å.

We have also explored the wings of the Ly $\alpha$   $\lambda 1216$  and MgII  $\lambda 2800$  (see fig. 5), but no other obvious absorption lines are evident.

**Table 3.** Details of *ROSAT* observations of H1419+480, along with expected values of the PSPC Hardness Ratio and Softness ratios derived from the best-fit to the *XMM-Newton* data with and without the OVII edge.

Parameter	<i>ROSAT</i> (RASS)	<i>ROSAT</i> (ROR700038)	<i>XMM-Newton</i> (with OVII edge)	<i>XMM-Newton</i> (without OVII edge)
Exposure time (s)	375	1266		
Flux <sup>a</sup>	$7 \times 10^{-12}$	$3 \times 10^{-12}$	$4.5 \times 10^{-12}$	$4.5 \times 10^{-12}$
<i>HR</i> <sup>b</sup>	$+0.0 \pm 0.1$	-	$+0.11$	$+0.14$
<i>SR</i> <sub>1</sub> <sup>c</sup>	-	$+1.6 \pm 0.2$	$+2.0$	$+1.8$
<i>SR</i> <sub>2</sub> <sup>d</sup>	-	$+0.7 \pm 0.1$	$+0.5$	$+0.6$

<sup>a</sup> Flux in the 0.5-2 keV band in units of  $\text{erg cm}^{-2} \text{s}^{-1}$ , corrected for Galactic absorption using the best fit model from table 1

<sup>b</sup> PSPC Hardness Ratio  $HR = (H - S)/(H + S)$  where  $S$  and  $H$  are the counts detected in PSPC channels 11-39 and 50-200 respectively.

<sup>c</sup> PSPC softness ratio  $SR_1 = S_1/H_1$ , where  $S_1$  and  $H_1$  are the counts detected in PSPC channels 11-39 and 40-85 respectively.

<sup>d</sup> PSPC softness ratio  $SR_2 = S_2/H_2$ , where  $S_2$  and  $H_2$  are the counts detected in PSPC channels 40-85 and 86-200 respectively.

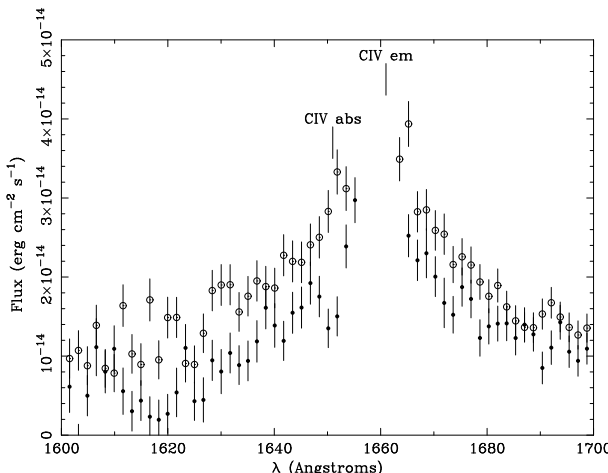


**Figure 4.** IUE/SWP spectra of H1419+480 around the CIV emission line. Only datapoints which have not been flagged by any reason are plotted. Filled (hollow) circles are from the SWP17265 (SWP18951) observations respectively.

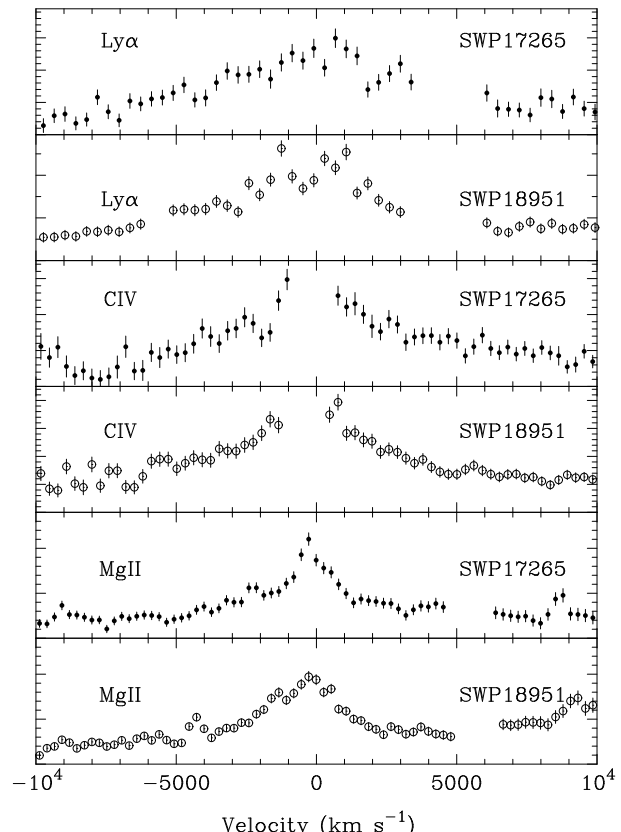
**Table 4.** Details of IUE/SWP observations of H1419+480.

Image identification	Date	Exposure (s)
SWP17265	1982-06-19	8400
SWP18951	1983-01-05	9000

#### 4 HAVE THE X-RAY AND UV ABSORBERS A COMMON ORIGIN?

In order to find out whether the ionized absorber seen in the *XMM-Newton* X-ray data and the associated UV absorber seen in the IUE data could be produced by photoionized gas, we must first determine the parameters of the CIV absorption line and then compare them with the expectations from the X-ray warm absorber. Indeed both absorbers are seen to vary with time, but the aim here is to see whether the absorption could arise in the same changing photoionised gas cloud.

At the 6Å resolution of this setup, the CIV doublet ( $\lambda\lambda 1548, 1550$ ) is unresolved and, obviously, we cannot measure directly the absorbing column density. Fig 6 shows the curve of growth (i.e., equivalent width versus column density) for the whole CIV doublet and a range of velocity dis-



**Figure 5.** IUE/SWP velocity spectra of H1419+480 around the Ly $\alpha$ , CIV and MgII emission lines. Only datapoints which have not been flagged by any reason are plotted. Filled (hollow) circles are from the SWP17265 (SWP18951) observations respectively.

persion parameters. As usual a Voigt profile has been assumed for each line in the doublet, with velocity width parameter  $b = \sqrt{2}\sigma$  ( $\sigma$  is the velocity dispersion of the gas, assumed Maxwellian), damping constant  $2.64 \times 10^8 \text{ s}^{-1}$  and a total oscillator strength of 0.28 (which is the sum of the oscillator strengths for the two lines). The approximation introduced by Whiting (1968) to the Voigt profile (accurate to better than 5%) has been used.

In order to compare the properties of this associated absorption line with those of the X-ray ionized absorber, we have computed the expected CIV column density ( $N_{\text{CIV}}$ )

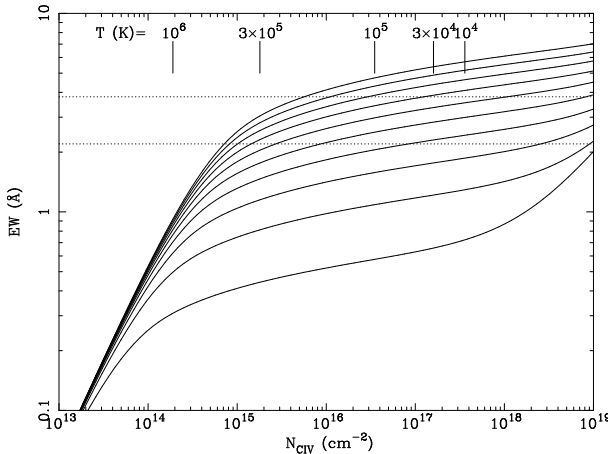


**Figure 6.** Curve of growth for the CIV  $\lambda\lambda 1548,1550$  doublet (continuous lines). Velocity dispersion parameters  $b = \sqrt{2}\sigma$  ( $\sigma$  is the velocity dispersion of the gas) range from 20 to 200  $\text{km s}^{-1}$  in steps of 20  $\text{km s}^{-1}$  from bottom to top. The dotted lines show the measured equivalent width formal 90% confidence interval. Vertical marks denote the expected column density for a range of temperatures of the absorber.

for the absorber temperatures listed in table 2 and using the corresponding ionisation parameter. To this goal, **XSTAR** (version 2.1h) has been used, along with solar abundances. Results have not seen to vary significantly for a wide range of gas densities ( $1 - 10^{10} \text{ cm}^{-3}$ ). The values obtained for  $N_{\text{CIV}}$  and  $N_{\text{HI}}$  are listed in the last columns, while the values for  $N_{\text{MgII}}$  are always below  $10^{13} \text{ cm}^{-2}$  and therefore undetectable. The values of  $N_{\text{CIV}}$  are also overlayed in fig. 6.

Unfortunately, the constraints emerging by matching the properties of the X-ray absorber and of the CIV absorption feature are very weak, as we are in the flat (saturated) part of the curve of growth. It is clear, though, that at temperatures close to  $10^6 \text{ K}$  or higher, the C atoms are almost fully ionised and it is difficult to produce an equivalent width of the order of a few Å. At a temperature below  $\sim 10^5 \text{ K}$ , the implied CIV column is larger than  $3.5 \times 10^{16} \text{ cm}^{-2}$  and the Doppler velocity width  $b < 100 \text{ km s}^{-1}$ . These temperatures are not favoured by the X-ray analysis (see Section 2). In addition, the HI Ly $\alpha$  line would be as strong as the CIV doublet under these conditions (see table 2 again) and difficult to miss in the IUE spectrum. These arguments favour a temperature for the absorber of a few  $\times 10^5 \text{ K}$  and column density  $N_{\text{CIV}} < 10^{16} \text{ cm}^{-2}$ .

Mathur et al (1994) performed a detailed study of the warm absorber in 3C 351, where a strong CIV associated absorber was found (equivalent width  $\sim 3 \text{ Å}$ ). The simultaneous modeling of various lines of the same UV absorber yielded moderate values of  $N_{\text{CIV}} \sim 10^{16} \text{ cm}^{-2}$  and  $b$  around  $100 \text{ km s}^{-1}$  for that system, very much along the lines that we suggest for the absorber towards H1419+480.

## 5 CONCLUSIONS

The bright Seyfert 1 galaxy H1419+480 has been shown to be variable in X-rays by comparing our *XMM-Newton* observations with earlier *ROSAT* data. A warm absorber is clearly seen (mostly through the OVII K-edge) in the *XMM*-

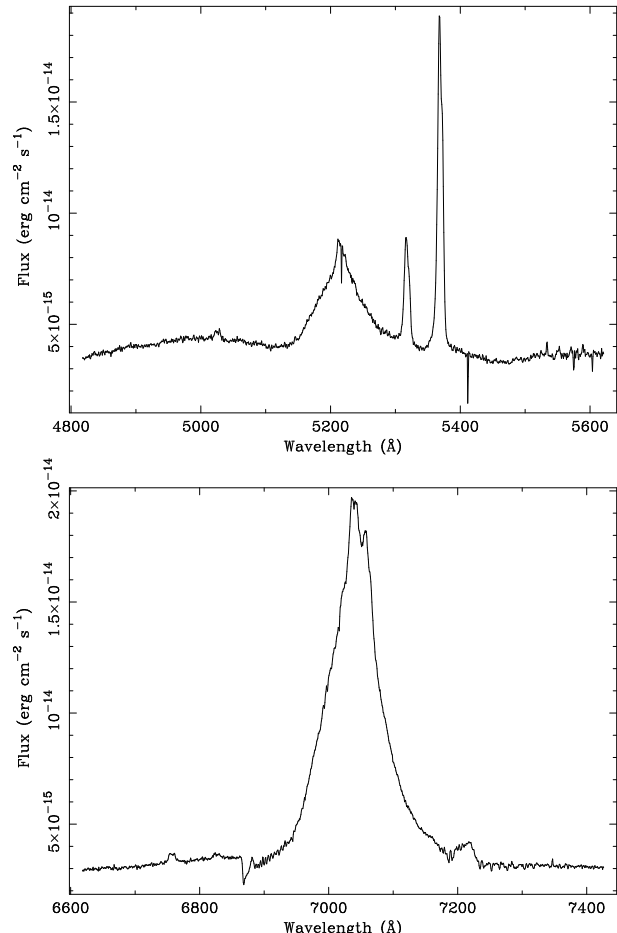


**Figure 7.** Optical spectrum of H1419+480.

*Newton* data, but there are hints that it was either weaker or absent in the *ROSAT* observation of 1992.

Further, an IUE observation of H1419+480 conducted in 1983 shows  $\sim 3\sigma$  evidence for a CIV associated absorber, outflowing with a velocity  $\sim 1800 \text{ km s}^{-1}$ . This absorption line was not present in an observation taken roughly 1 year before. The variability of this associated line implies a size  $D$  of the absorbing gas of the order of a pc or less. Assuming that the UV and X-ray absorbers have a common origin, we can estimate the distance to the nucleus  $R$  by using the ionisation parameter, measured luminosity and well-determined total column density around  $2.5 \times 10^{21} \text{ cm}^{-2}$

$$R \approx 200 D(\text{pc})^{1/2} \xi^{-1/2} \text{ pc},$$

i.e.,  $R \sim 100 \text{ pc}$ .

In conclusion, the gas that produces the X-ray and the UV absorption can be explained within a common origin. In this case the gas should be located  $\sim 100 \text{ pc}$  away from the nucleus, with a temperature of a few  $\times 10^5 \text{ K}$  and the size of the gas cloud should be  $\sim 1 \text{ pc}$ .

## APPENDIX A: THE OPTICAL SPECTRUM OF H1419+480

H1419+480 was observed in the 4.2m William Herschel Telescope at the Observatorio del Roque de Los Muchachos in

the island of La Palma (Canary Islands, Spain), on February 26, 1998. We used the ISIS double spectrograph with 600 line/mm gratings on both the blue and red arms, with the wavelengths centered at 5200 and 7000 Å respectively, in order to observe the H $\beta$ +[OIII] region in the blue and the H $\alpha$ +[NII]+[SII] in the red. Weather conditions were good and probably photometric, but the seeing was around 1.5 arcsec. Two 300 sec observations (co-added in the reduction process) were carried out with the slit aligned to parallactic angle. For details on the reduction process, see Barcons et al (2003) as the same setup and procedure was used.

Fig. 7 shows the optical blue and red spectrum of H1419+480. The [OIII] lines have some structure, with two peaks separated  $\sim 60$  km s $^{-1}$ . This is the main limiting factor in the precision of the redshift, that we measure by fitting both lines to a common redshift and find  $z = 0.072296 \pm 0.000004$ .

## ACKNOWLEDGEMENTS

The work reported herein is based partly on observations obtained with *XMM-Newton*, an ESA science mission with instruments and contributions directly funded by ESA member states and the USA (NASA). It is also based on INES data from the IUE observatory. We thank Enrique Solano for assistance with the INES data. The *WHT* telescope is operated by the Isaac Newton Group on the Spanish Observatorio del Roque de los Muchachos of the Instituto de Astrofísica de Canarias. We acknowledge financial support by the Ministerio de Ciencia y Tecnología (Spain), under grants AYA2000-1690 and ESP2001-4537-PE.

## REFERENCES

Arnaud K.A., 1996, In ASP Conference Series, Vol 101, 17  
 Barcons X., Carrera F.J., Ceballos M.T., 2003, MNRAS, 339, 757  
 Branduardi-Raymont G., Sako M., Kahn S.M., Brinkman A.C., Kaastra J.S., Page M.J., 2001, A&A, 365, L140  
 Ceballos M.T., Barcons X., 1996, MNRAS, 282, 493  
 Crenshaw D.M., Kraemer S.B., Bogges A., Maran S.P., Mushotzky R.F., Wu C.-C., 1999, ApJ, 516, 750  
 den Herder J.W., et al., 2001, A&A, 365, L7  
 Fabian A.C. et al , 1994, PASJ, 46, L59  
 George I.M., Turner T.J., Netzer H., Nandra K., Mushotzky R.F., Yaqoob T., 1998, ApJS, 114, 73  
 Halpern J.P., 1984, ApJ, 281, 90  
 Jansen F.A., et al., 2001, A&A, 365, L1  
 Lee J.C., Ogle P.M., Canizares C.R., Marshall H.L., Schulz N.S., Morales R., Fabian A.C., Iwasawa K., 2001, 554, L13  
 Mason K.O., et al., 2001, A&A, 365, L36  
 Mason K.O., et al., 2003, ApJ, 582, 95  
 Mathur S., 1994, ApJ, 431, L75  
 Mathur S., Wilkes B., Elvis M., Fiore F., 1994, 434, 493  
 Mathur S., Elvis M., Wilkes B., 1995, ApJ, 452, 230  
 Nandra K., Pounds K.A., 1992, Nat, 359, 21  
 Nandra K., Pounds K.A., 1994, MNRAS, 268, 405  
 Otani C., et al., 1996, PASJ, 48, 211  
 Remillard R. ,Bradt H.V.D., Brissenden R.J.V., Buckley D.A.H., Roberts W., Schwartz D.A., Stroozas B.A., Tuohy I.R., 1993, AJ, 105, 2079  
 Reynolds C.S., Fabian A.C., 1995, MNRAS, 273, 1167  
 Reynolds C.S., 1997, MNRAS, 286, 513  
 Schwope A., et al, 2000, AN, 321, 1  
 Strüder L., et al., 2001, A&A, 365, L18  
 Turner M.J.L. et al., 2001, A&A, 365, L27  
 Whiting E.E., 1968, J. Quant. Spectrosc. Rad. Transf., 8, 1379  
 Wood K.S., et al., 1984, ApJS, 56, 507

This paper has been typeset from a *TeX/ L<sup>A</sup>TeX* file prepared by the author.